

Improved Emitter Transit Time Using AlGaAs–GaInP Composite Emitter in GaInP/GaAs Heterojunction Bipolar Transistors

Jae-Woo Park, *Member, IEEE*, Dimitris Pavlidis, *Fellow, IEEE*, Saeed Mohammadi, *Member, IEEE*, Jean-Luc Guyaux, and Jean-Charles Garcia

Abstract—A new emitter structure based on composite graded AlGaAs–GaInP approach is described, which allows significant reduction of C_{BE} and improved high-frequency performance. A theoretical study of the composite and conventional emitter HBTs is performed to prove the superiority of composite emitter HBTs using Monte Carlo simulation of their transport properties. The self-aligned HBTs fabricated in this study are grown by CBE with TBA/TBP precursors. The current gain cutoff frequency (f_T) was 62 GHz for the composite emitter design HBT, and 45 GHz for conventional emitter design HBT. The C_{BE} achieved with the composite emitter designs was by at least 3 times lower than that of conventional designs and does not show significant variation with collector current. This leads to enhanced f_T characteristics by 15% for composite emitter HBT designs and confirms the theoretical expectations.

Index Terms—GaAs, heterojunction bipolar transistors (HBTs), Monte Carlo simulation, transit time.

I. INTRODUCTION

FOR long-haul optical communication systems, ultra-broadband, high bit rate front-end transimpedance amplifiers are needed. 40 Gb/s-class ICs using AlGaAs HBTs have already been demonstrated [1], [2]. GaInP/GaAs heterojunction bipolar transistors (HBTs) grown by MOCVD have been first demonstrated by the authors [3], and this technology is currently accepted as a superb alternative to AlGaAs/GaAs HBTs due to the absence of Al, the excellent etching selectivity, and better reliability characteristics [4], [5]. Monolithic broadband GaInP/GaAs HBT transimpedance amplifiers having a bandwidth (BW) of 19 GHz have been demonstrated by the authors and their large signal, as well as, a high gain performance have been reported [6], [7]. Excellent microwave performance of $f_T = 140$ –GHz and $f_{max} = 230$ GHz has been achieved using GaInP/GaAs HBTs [8], and chemical beam epitaxy (CBE) using TBA/TBP precursors has been reported for growth of GaInP/GaAs devices [9]. High-speed microwave performance of GaInP/GaAs HBTs can be achieved using various designs

such as tunneling emitter [10], strained InGaAs base [11], and collector undercut [12]. A common limitation in high speed performance of HBTs has been their relatively large base-emitter capacitance (C_{BE}), which results from limited mobile carrier transport and thus charges accumulation in the emitter region [13]. The use of lightly doped emitter with δ -doping was reported to reduce C_{BE} at low current density [14], but this does not resolve the problem at high current density where C_{BE} is considerably increased. As expected, a tradeoff exists in the relation between R_{BE} and C_{BE} for high speed performance since R_{BE} is decreased as the collector current (I_C) increases, while at same time C_{BE} is increased. This tradeoff imposes a difficulty in reducing the emitter transit time (τ_E) and thus enhancing the device microwave performance. The emitter transit time of an HBT can be estimated analytically using the following expression:

$$\tau_E = \frac{kT}{qJ_C}(C_{BE} + C_{BC}) = \frac{kT}{qJ_C} \left(\frac{\Delta Q_e}{\Delta V_{BE}} + C_{BC} \right) \quad (1)$$

where

- τ_E emitter transit time of the device;
- kT/qJ_C transconductance;
- C_{BE} base-emitter capacitance;
- C_{BC} base-collector capacitance;
- Q_e electron charge in the emitter region.

Since usually the base-emitter capacitance (C_{BE}) is much larger than the base-collector capacitance (C_{BC}), the first term of (1) is simplified to $R_{BE}C_{BE}$. Mobile carrier transport takes place in conventional emitter HBT designs by diffusion and results in charge accumulation in the emitter and thus increased C_{BE} . In this work, a composite AlGaAs/GaInP emitter design was employed to reduce the impact of this effect following the approach originally reported by [15]. While the improved HBT performance presented in [15] was only shown theoretically, first experimental results on HBTs designed with this approach were demonstrated by the authors [16] and further theoretical and experimental validation of this concept is reported in this paper.

In the design presented here, a compositionally graded AlGaAs layer forms an electron launcher at the interface with the GaInP layer, which injects the electrons at a high kinetic energy toward the remaining part of the emitter. It leads to lower free carrier concentration (Q_e) and smaller C_{BE} compared to a conventional emitter design approach, even under high current operation conditions. The low free carrier concentration in the emitter is achieved

Manuscript received February 1, 2000; revised January 29, 2001. This work was supported in part by Thomson-CSF, CNET France-Telecom/DRI Contract 94 6M 917 and MURI Contract DAAH04-96-1-0001. The review of this paper was arranged by Prof. A. S. Brown.

J.-W. Park is with Knowledge-on Enyang-dong, Seoul, Korea.

D. Pavlidis and S. Mohammadi are with the Department of Electrical Engineering and Computer Science, University of Michigan, Ann Arbor, MI 48109-2122 USA.

J.-L. Guyaux and J.-C. Garcia are with the Central Research Laboratory, Thomson-CSF, 91404 Orsay, France.

Publisher Item Identifier S 0018-9383(01)05559-9.

without any transconductance degradation, due to the high electron velocity in the electron launcher region. As a result, an overall performance improvement compared to conventional emitter design is achieved. This paper provides an analysis of the emitter and total delay times in HBTs and demonstrates the advantages of using electron launcher region in the emitter for reduction of these delay times. Theoretical and experimental verifications of the improved delay times are shown using Monte Carlo simulation and through device characterization and small-signal modeling. Furthermore, it is shown that the reported composite emitter HBT design using the AlGaAs/GaInP approach achieves reduced C_{BE} and improved high-frequency performance over a broad collector current range.

II. MONTE CARLO STUDY OF THE COMPOSITE EMITTER DESIGN

Graded AlGaAs–GaInP composite emitter design HBTs were studied using Monte Carlo simulations. This allowed evaluation of transistor band structure, electric field, velocity profile and carrier distribution. The latter provided information on charge changes with current, which are indicative of emitter transit time τ_E as will be discussed in this section. As discussed earlier, the graded AlGaAs layer introduced in the composite emitter design is important for reducing the emitter charging time (τ_E). This layer forms an electron launcher at the interface with the GaInP layer as shown in Fig. 1(a). The launcher injects electrons into the GaInP region with elevated kinetic energy. This ensures high-energy electron transport through the GaInP emitter and results in overshoot velocity before carriers start being injected into the base, leading to a lower free carrier concentration in the emitter and thus lower τ_E . The role of GaInP emitter layer in the composite emitter structure is to block the holes from back-injecting into the emitter and separate the launcher from the base, giving a reduced emitter-base capacitance (C_{BE}). Fig. 1 shows the energy-band diagrams and layer structure of GaInP/GaAs composite (a) and conventional (b) emitter design HBTs studied in this work. In case of the GaInP/GaAs conventional emitter design HBT, a 800 Å thick GaInP emitter layer is added to allow comparison with AlGaAs–GaInP composite emitter design HBTs of same overall emitter thickness. Since the energy separation between the Γ band and L band in GaInP is small ($\Delta E_{TL} = 0.153$ eV), the Al composition (x) at the AlGaAs–GaInP interface must be chosen properly to avoid intervalley scattering.

In this study, an Al composition (x) of 0.22 was chosen to prevent the intervalley scattering. This composition yields an electron launcher with a height of 0.125 eV. Fig. 2 shows (a) the electric field and (b) electron density versus distance profiles for GaInP/GaAs conventional and AlGaAs–GaInP composite emitter design HBTs. Compositionally graded AlGaAs emitter HBTs have much stronger electric fields present in the emitter. A maximum value of 40 kV/cm is for example observed within the AlGaAs region of the composite design, while no electric field is present in the emitter of the conventional design. The corresponding electron density is therefore dramatically decreased due to the presence of a drift velocity component in this region of the emitter. On the other hand, GaInP conventional

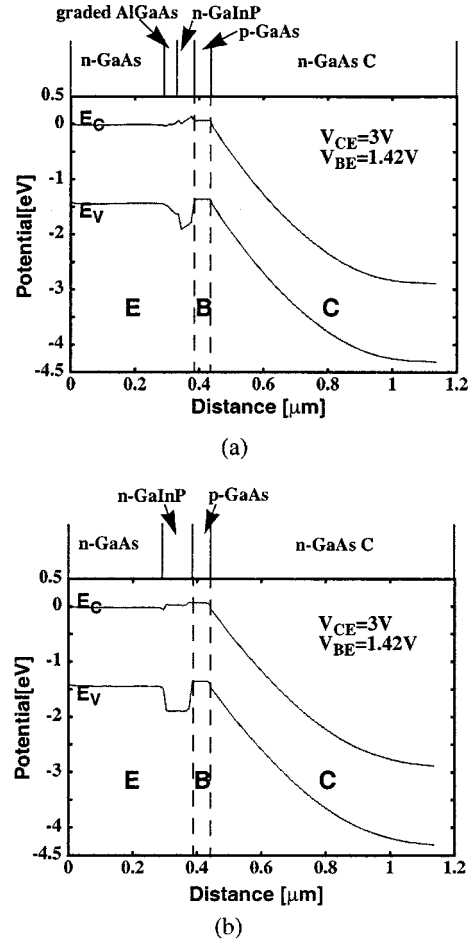
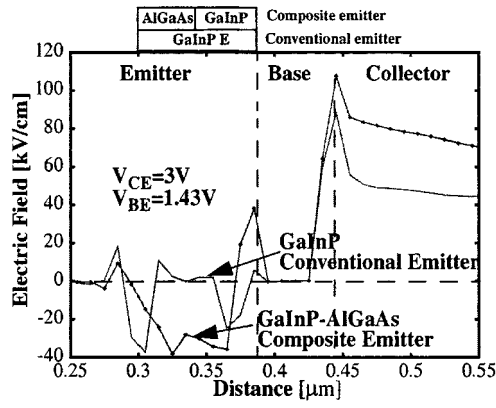


Fig. 1. Energy band diagrams of GaInP/GaAs (a) conventional and (b) composite emitter design HBTs.

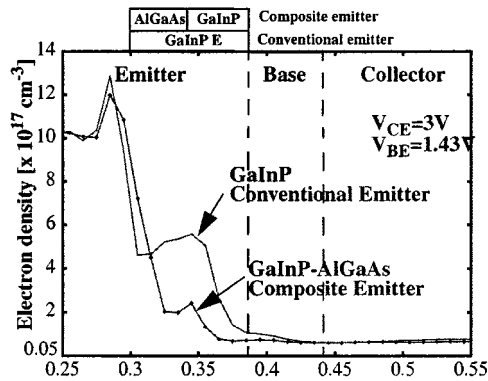
emitter HBTs do not have a built-in electric field within the emitter region, and the electron density in this case is increased due to slow transport of carriers and thus carrier accumulation. The enhancement of the drift velocity using the compositionally graded AlGaAs design can be better understood from the results of Fig. 3. This figure focuses on the velocity characteristics responsible for the improved frequency characteristics reported in the paper. In case of the composite emitter design, the electron velocity is high due to the drift velocity component in the special emitter region. On the contrary, the electron velocity of the conventional emitter design is slower than for the composite emitter design since diffusion carrier transport is dominant in the emitter region, which consists only of GaInP. One sees from these simulations that C_{BE} for the composite emitter design HBT is expected to be smaller than for the conventional emitter HBT due to the stronger electric field in the composite emitter region. This leads to reduced $\tau_E(\Delta Q_e/\Delta J_C)$, which is an important parameter in determining the cutoff frequency $f_T = 1/\tau_{EC}$, where τ_{EC} is given by

$$\tau_{EC} \approx \tau_E + \tau_B + \tau_C + C_{BC}R_C \quad (2)$$

and τ_E can be evaluated from $\tau_E \approx \Delta Q_e/\Delta J_C = C_{BE}R_{BE}$. An estimate of τ_E for the two designs using Monte Carlo simulation to evaluate $\Delta Q_e/\Delta J_C$ showed values of 0.13 ps and 0.57 ps



(a)



(b)

Fig. 2. (a) Comparison of electric field and (b) electron density profiles for GaInP conventional and AlGaAs-GaInP composite emitter design HBTs.

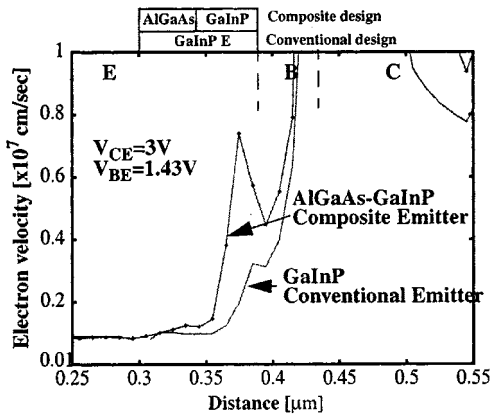
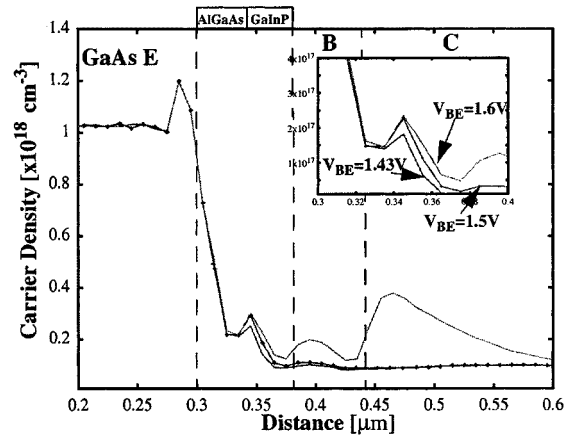


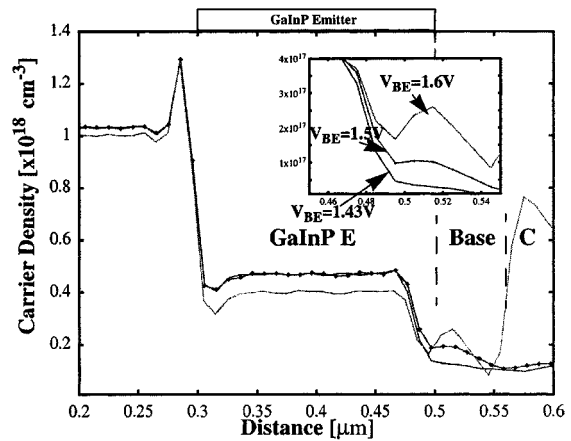
Fig. 3. Comparison of electron velocity profiles for GaInP conventional and AlGaAs-GaInP emitter design HBTs in the composite emitter region.

for the composite and conventional design, respectively, proving the superiority of the former.

The theoretically expected carrier density values for designs employing the same concept can be found in Fig. 4. The thickness and doping concentration (800 Å versus 2000 Å and 5×10^{16} versus 3×10^{17} cm⁻³ for composite and conventional emitters, respectively) of the emitter layer employed in this simulation correspond to those of the fabricated HBTs. As shown in the inset of Fig. 4(a), the increase in the free electron con-



(a)



(b)

Fig. 4. Bias dependence of free electron carrier density (a) for the composite and (b) the conventional emitter design HBTs.

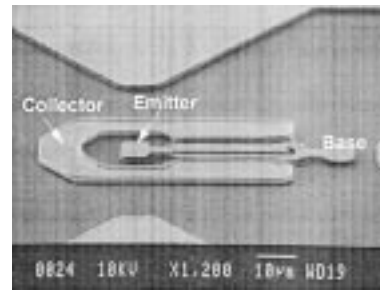


Fig. 5. SEM picture of the fabricated $2 \times 30 \mu\text{m}^2$ single emitter GaInP/GaAs HBT.

centration (ΔQ_e) at the base-emitter junction of the composite emitter design due to V_{BE} increase is small, whereas the ΔQ_e increase in the conventional design [see the inset of Fig. 4(b)] is significant. The difference in the ΔQ_e values is again due to the presence of a stronger electric field and thus higher electron velocity in the vicinity of the base-emitter junction of the composite emitter design compared to the conventional design.

III. LAYER STRUCTURE AND DEVICE FABRICATION

The GaInP/GaAs HBT layers were grown by CBE using reduced toxicity precursors such as TBA and TBP. The details

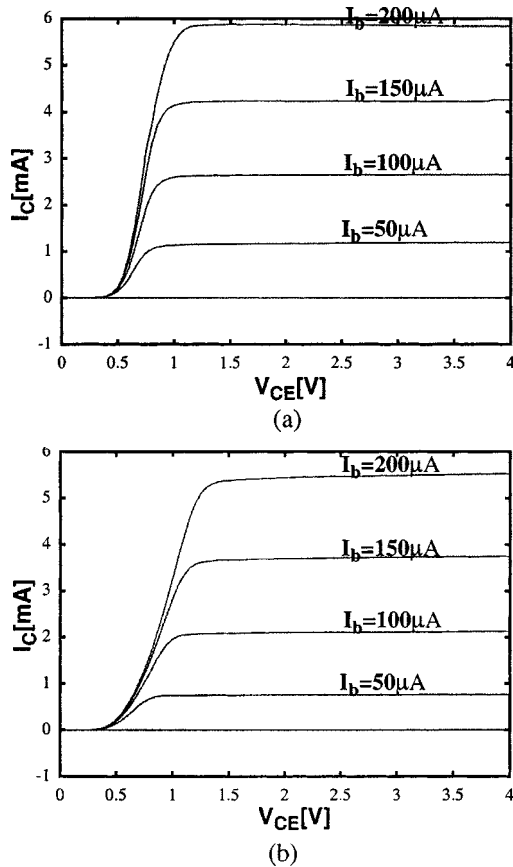


Fig. 6. (a) DC characteristics of composite emitter and (b) conventional emitter design HBTs.

of the growth technique and material characteristics were described by the authors [9], [17]. The composite emitter HBT design consists of a compositionally graded $5 \times 10^{17} \text{ cm}^{-3}$, 380 Å thick AlGaAs (Al : 0 → 0.22) layer followed by undoped 100 Å thick GaInP, which serves in reducing the spike created in the conduction band of the AlGaAs–GaInP heterointerface. A 400 Å thick n ($5 \times 10^{16} \text{ cm}^{-3}$) GaInP emitter layer is used below the undoped GaInP and a 500 Å GaAs base doped p^+ ($6 \times 10^{19} \text{ cm}^{-3}$) and a 7000 Å GaAs collector n^- ($1.5 \times 10^{16} \text{ cm}^{-3}$). To better evaluate the advantages of the composite emitter design and validate the proposed approach, an abrupt junction GaInP/GaAs conventional HBT was also fabricated for comparison. The emitter design of the conventional HBT consists, starting from the emitter cap, of an n^+ ($1 \times 10^{19} \text{ cm}^{-3}$) GaInP, 700 Å thick layer followed by 2000 Å thick GaInP emitter doped n ($3 \times 10^{17} \text{ cm}^{-3}$), a 600 Å GaAs base doped p^+ ($4 \times 10^{19} \text{ cm}^{-3}$), and a 7000 Å GaAs collector n^- ($1.5 \times 10^{16} \text{ cm}^{-3}$). The emitter doping and thickness ($3 \times 10^{17} \text{ cm}^{-3}$, 2000 Å) of the conventional HBT were optimized for sufficient DC gain and high frequency performance. A common design feature of the two HBT structures is a GaInP etch stop layer between the GaAs collector and subcollector. This can be used to form a laterally etched undercut and leads to reduction of the C_{BC} capacitance and thus cutoff frequency as well as maximum oscillation frequency enhancement [17]. Self-aligned HBTs with single $2 \times 30 \mu\text{m}^2$ emitter fingers were fabricated on the above layers and a photograph of a device before airbridge metal realization is shown in Fig. 5. The key

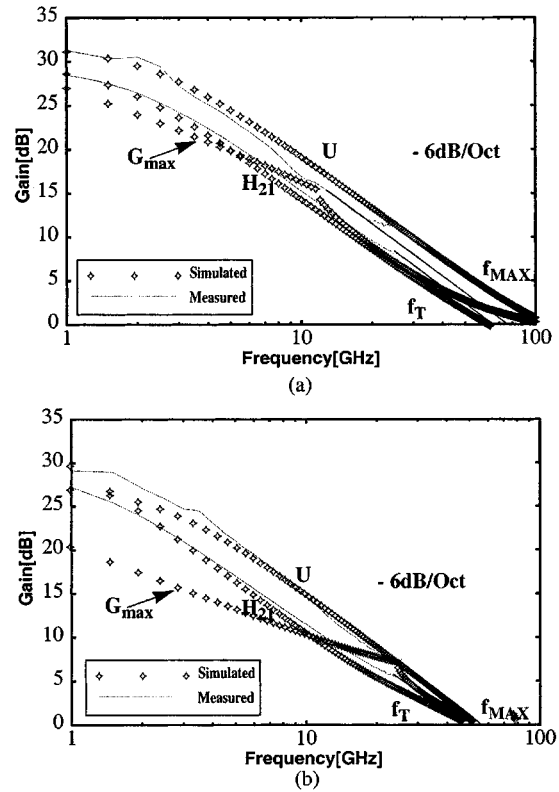


Fig. 7. Measured and simulated microwave performance of composite emitter (a) and conventional emitter (b) design HBTs.

process features are as follows: Ti/Pt/Au nonalloyed emitter and collector ohmic contacts, Pt/Ti/Pt/Au nonalloyed base contacts, and GaInP emitter etch by HCl and pillar/airbridge fabrication using Ti/Al/Ti/Au. GaAs collector undercut as necessary for reducing C_{BC} was achieved by a wet etching solution consisting of $\text{NH}_4\text{OH} : \text{H}_2\text{O}_2 : \text{H}_2\text{O}$. A cross-sectional view of a completed HBT with laterally etched undercut can be found in a previous report by the authors [17].

IV. EXPERIMENTAL RESULTS AND ANALYSIS

A. DC and Microwave Performance

The dc characteristics of $2 \times 30 \mu\text{m}^2$ single emitter finger HBTs with the composite and conventional emitter designs were measured using an HP4145B semiconductor parameter analyzer. Fig. 6 shows the I – V characteristics of the fabricated $2 \times 30 \mu\text{m}^2$ single emitter finger GaInP/GaAs HBTs for the composite and conventional emitter devices. A dc gain of 30 and 28, base ideality factors of 1.74, 1.82 and collector ideality factors of 1.15, 1.18 and a collector-emitter breakdown voltage of above 17 V, are obtained for the composite emitter and conventional emitter device, respectively.

The microwave properties of HBTs were measured in common-emitter configuration using on wafer tests and an HP8510B network analyzer. The current and power gain versus frequency characteristics of the composite emitter HBT are shown in Fig. 7. The current gain cutoff frequency (f_T) extrapolated from the measured $|H_{21}|$ using a -6 dB/Oct . slope rule was 62 GHz for the composite emitter design HBT, and 45 GHz

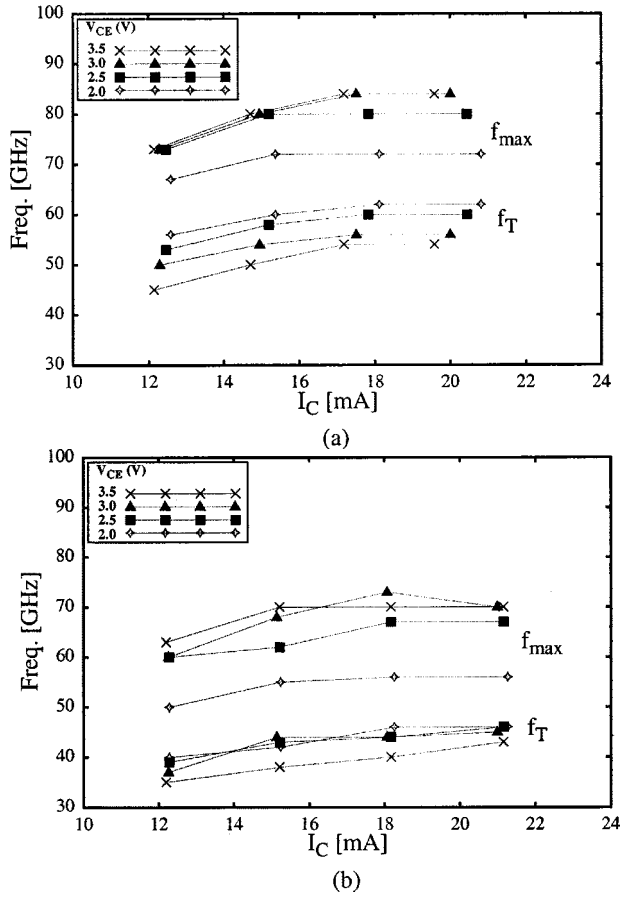


Fig. 8. Bias dependence of microwave performance of (a) composite emitter and (b) conventional emitter design HBTs.

for conventional emitter design HBT. The maximum oscillation frequency (f_{max}) from Mason's unilateral gain (U) was 72 GHz at $V_{CE} = 2.0$ V, $I_C = 18$ mA for the composite emitter design and 55 GHz at $V_{CE} = 2.0$ V, $I_C = 18$ mA for the conventional emitter design. Comparison of the microwave performance of the composite emitter and the conventional emitter design shows that the f_T of the composite emitter design is by 38% higher. f_T and f_{max} were also evaluated from the small-signal HBT equivalent circuit parameters, and the results are also shown in Fig. 7. The f_T , f_{max} values found using this approach were 63 GHz and 120 GHz for the composite emitter design and 45 and 60 GHz for the conventional emitter design, respectively. Although the f_{max} of the composite HBT obtained from this technique is higher than the one obtained by extrapolation (120 GHz versus 72 GHz), the overall trends are the same and demonstrate the superiority of composite emitter HBTs.

Fig. 8 shows bias dependence of f_T and f_{max} as a function of collector current for the two design HBTs. In case of the composite emitter design, the peak f_T and f_{max} are 63 GHz at $V_{CE} = 2$ V, $I_C = 21.5$ mA and 84 GHz at $V_{CE} = 3$ V, $I_C = 20$ mA, respectively. The enhanced f_T characteristics at high collector current region obtained for composite emitter HBT [Fig. 8(a)] are due to its overall smaller C_{BE} value. The higher f_T of the composite emitter HBTs at low I_C appears to be related to their smaller C_{BE} which results from the lower emitter doping concentration in the composite emitter HBT ($n = 5 \times$

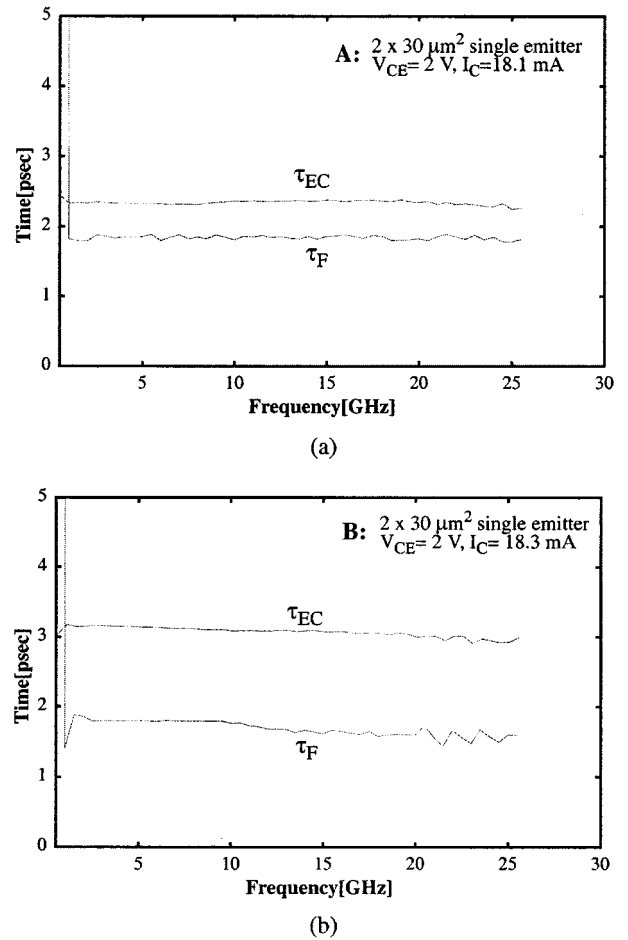


Fig. 9. Comparison of delay time of composite emitter and conventional emitter design HBTs.

10^{16} versus $n = 3 \times 10^{17}$). It will be analyzed and discussed in more detail in the next section.

B. Device Analysis and Discussion

The HBT small-signal equivalent circuit parameters were directly extracted from measured S parameter data using an in-house analytical extraction technique based on a technique that was previously reported [18]. The total delay time (τ_{EC}) and forward transit time ($\tau_F = \tau_B + \tau_C$) were calculated analytically from the impedance block elements of the HBT equivalent circuit. The relations below summarize the approach used [13], [18]

$$\tau_{EC} = \tau_E + \tau_B + \tau_C + \tau'_C = \text{ang} \frac{[Z_{12} - Z_{21}]}{[Z_{22} - Z_{21}]} \quad (3)$$

$$\tau_F = \tau_B + \tau_C = \tan^{-1} \frac{\text{Re}[\alpha Z_{BC}]}{\text{Im}[\alpha Z_{BC}]} \quad (4)$$

where

$$\tau_E \approx R_{BE}(C_{BE} + C_{BC}) \quad (5)$$

$$\tau'_C = C_{BC}(R_E + R_C) \quad (6)$$

and Z_{ij} is an impedance matrix, Z_{BC} is the impedance value of C_{BC} , α is the base transport factor, and τ_F is the forward transit time.

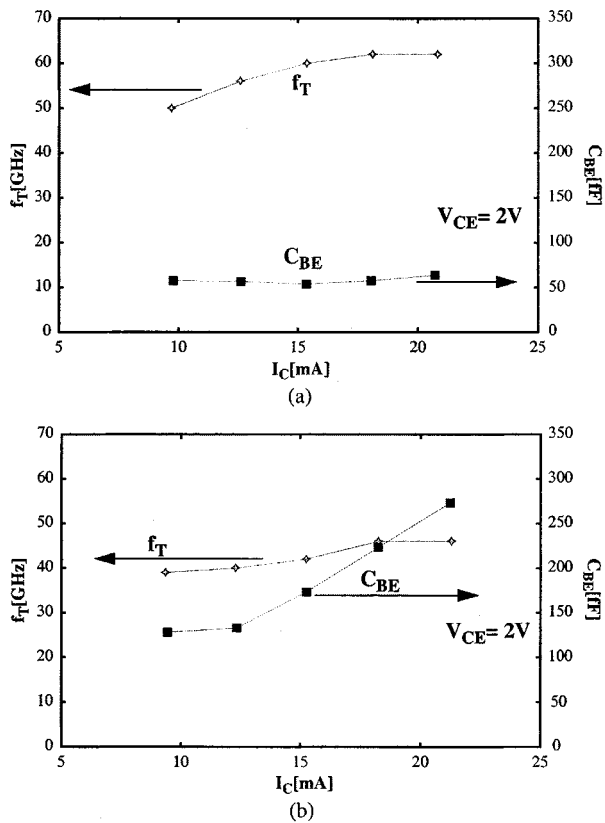


Fig. 10. Comparison of C_{BE} and f_T characteristics with collector current.

The calculated τ_{EC} , τ_F as function of frequency from the extracted small signal parameters are shown in Fig. 9. In case of the composite emitter design, a τ_{EC} of 2.33 ps and a τ_F of 1.8 ps were achieved, which leads to an emitter delay time ($\tau_E = \tau_{EC} - \tau_F - \tau'_C$) of only 0.22 p. $\tau'_C = C_{BC}(R_E + R_C)$ was in this case 0.31 ps. On the other hand, the total delay time (τ_{EC}) of the conventional emitter design was 3 ps while its forward transit time (τ_F) was 1.8 p. The resulting emitter delay time (τ_E) for the conventional emitter design was consequently 0.62 ps. These results indicate that the emitter delay time of the composite emitter design leads to enhancement of cutoff frequency which in the case of the tested devices is of the order of 15%. The C_{BE} and f_T dependence on J_C manifests distinct features for composite and conventional emitter designs as shown in Fig. 10 for a $2 \times 30 \mu\text{m}^2$ single emitter device. The C_{BE} values shown in this figure were obtained experimentally using (5) and (6), from which one finds $C_{BE} = (\tau_E/R_{BE}) - C_{BC}$. In particular, the C_{BE} of composite emitter HBTs is significantly lower than that of conventional emitter designs and presents a weak J_C dependence. This feature is representative of the composite emitter design and as expected from theory leads to enhanced f_T performance.

Fig. 11 illustrates that the C_{BE} and R_{BE} on collector current (I_C) at $V_{CE} = 2.0$ V for the composite and the conventional emitter GaInP/GaAs HBTs. R_{BE} was obtained experimentally using the relation

$$Re(Z_{BE} + Z_E) = R_{BE} + R_E \quad (7)$$

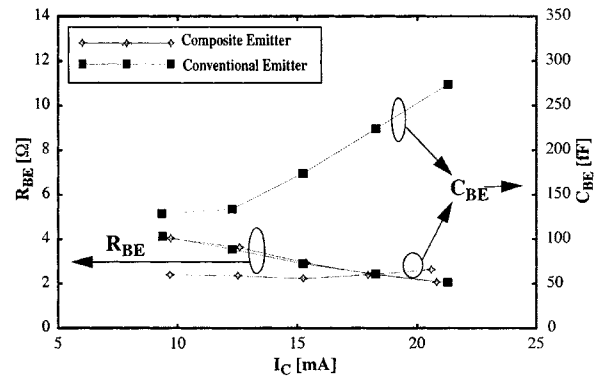


Fig. 11. C_{BE} and R_{BE} dependence on I_C for the composite and the conventional emitter GaInP/GaAs HBTs.

where R_E , Z_{BE} , and Z_E are also derived experimentally using the procedure developed by the authors and reported in [18]. As expected, C_{BE} for the composite emitter HBT is reduced by 55–77% compared with the conventional emitter HBT since the electron carrier density is dramatically decreased due to the high drift velocity in this region of the emitter. On the other hand, R_{BE} is a function of collector current (I_C) and has similar values for both designs over the entire range of investigated collector currents.

V. CONCLUSIONS

Self-aligned composite emitter AlGaAs–GaInP/GaAs HBTs were designed, fabricated, and analyzed. The composite emitter design HBTs showed superior characteristics in terms of reduced emitter-base capacitance (C_{BE}) and enhanced f_T performance. These results agree with simulated characteristics obtained by Monte Carlo. Experimental studies showed that f_T improved from 44 GHz to 62 GHz by using of the composite emitter design. Also, C_{BE} of the composite emitter design HBT was found to be at least three times lower than that of the conventional emitter design HBT under high I_C (J_C) bias operation conditions.

ACKNOWLEDGMENT

The authors would like to thank Prof. K. Tomizawa of Meiji University, Meiji, Japan, for stimulating discussions on HBTs.

REFERENCES

- [1] Y. Matsuoka and E. Sano, "High-speed AlGaAs/GaAs HBT's and their applications to 40Gbits/s-class IC's," in *IEEE GaAs IC Symp. Dig.*, 1994, pp. 185–188.
- [2] T. Otsuji, E. Sano, Y. Imai, and T. Enoki, "40-Gbit/s IC's for future light-wave communications systems," in *IEEE GaAs IC Symp. Dig.*, 1996, pp. 14–17.
- [3] M. Razeghi, F. Omnes, M. Defour, Ph. Maurel, J. Hu, and D. Pavlidis, "High performance GaAs/GaInP HBT's grown by MOCVD," *Sem. Sci. Technol.*, vol. 5, pp. 278–280, 1990.
- [4] G. I. Ng, D. Pavlidis, A. Samelis, D. Pehlke, J. C. Garcia, and J. P. Hirtz, "Demonstration of GaInP/GaAs HBT's grown with reduced toxicity all-metalorganic precursors," in *IEEE Int. Conf. Indium Phosphide and Related Materials*, 1994, pp. 399–402.
- [5] T. Takahashi, S. Sasa, A. Kawano, T. Iwai, and T. Fujii, "High-Reliability InGaP/GaAs HBT's Fabricated by Self-Aligned Process," in *Proc. IEEE Int. Electron Device Meeting (IEDM)*, San Francisco, CA, 1994, pp. 191–192.

- [6] J.-W. Park, S. Mohammadi, D. Pavlidis, C. Dua, J. Guyaux, and J. C. Garcia, "GaInP/GaAs HBT broadband monolithic transimpedance amplifiers and their high frequency small and large signal characteristics," in *IEEE MTT-S Int. Microwave Symp.*, 1998, pp. 39–42.
- [7] S. Mohammadi, J.-W. Park, D. Pavlidis, C. Dua, J. Guyaux, and J. C. Garcia, "High-gain GaInP/GaAs HBT monolithic transimpedance amplifier for high-speed optoelectronic receivers," in *Proc. IEEE Int. Electron Device Meeting (IEDM)*, San Francisco, CA, 1998, pp. 661–664.
- [8] S. Kobayashi, T. Fujita, T. Yakihara, S. Oka, and A. Miura, "Ultrahigh-speed InGaP/InGaAs HBT's using MG as the base dopant," in *Proc. Iridium Phosphide and Related Materials*, 1997, pp. 58–61.
- [9] J. C. Garcia, C. Dua, S. Mohammadi, J. W. Park, and D. Pavlidis, "Growth characterization of hydride-free CBE and application of GaInP/GaAs HBT's," *J. Electron. Mater.*, vol. 27, no. (5), pp. 442–445, May 1998.
- [10] C. C. Wu and S. S. Lu, "High performance InGaP/GaAs tunneling emitter bipolar transistors," *Jpn. J. Appl. Phys.*, vol. 32, pp. 560–562, 1993.
- [11] D. A. Ahmari, M. T. Fresina, Q. J. Hartman, D. W. Barlage, P. J. Mares, M. Feng, and G. E. Stillman, "High speed InGaP/GaAs HBT's with a strained InGaAs base," *IEEE Electron Device Lett.*, vol. 17, pp. 226–227, May 1996.
- [12] W. L. Chen, H. F. Chau, M. Tutt, M. C. Ho, T. S. Kim, and T. Henderson, "High-speed InGaP/GaAs HBT's using a simple collector undercut technique to reduce base-collector capacitance," *IEEE Electron Device Lett.*, vol. 18, pp. 355–357, July 1997.
- [13] J. M. M. Rios, L. M. Lunardi, S. Chandrasekhar, and Y. Miyamoto, "Self-consistent method for complete small-signal parameter extraction of InP-based heterojunction bipolar transistors," *IEEE Trans. Microwave Theory Tech.*, vol. 45, pp. 39–45, Jan. 1997.
- [14] C. E. Chang, P. M. Asbeck, L. T. Tran, D. C. Streit, and A. K. Oki, "Novel HBT structure for high f_T at low current density," in *IEDM Tech. Dig.*, 1993, pp. 795–798.
- [15] J. Hu, Q. M. Zhang, R. K. Surridge, J. M. Xu, and D. Pavlidis, "A new emitter design of InGaP/GaAs HBT's for high frequency applications," *IEEE Electron Device Lett.*, vol. 14, pp. 563–565, Dec. 1993.
- [16] J.-W. Park, D. Pavlidis, S. Mohammadi, C. Dua, and J. C. Garcia, "Improved high frequency performance by composite emitter Al-GaAs/GaInP HBT's fabricated using CBE," in *Proc. 24th Int. Symp. Compound Semiconductor*, San Diego, CA, 1997, pp. 439–442.
- [17] J.-W. Park, D. Pavlidis, S. Mohammadi, J. L. Guyaux, and J. C. Garcia, "Material and processing technology for manufacturing of high speed, high reliability GaInP/GaAs HBT based IC's," in *Int. Conf. GaAs Manufacturing Technology*, Vancouver, BC, Canada, 1999, pp. 173–176.
- [18] D. R. Pehlke and D. Pavlidis, "Evaluation of the factors determining HBT high-frequency performance by direct analysis of S-parameter data," *IEEE Trans. Microwave Theory Tech.*, vol. 40, pp. 2367–2373, Dec. 1992.

Jae-Woo Park (S'88–M'92), photograph and biography not available at the time of publication.



Dimitris Pavlidis (S'73–M'76–SM'83–F'93) received the B.Sc. degree in physics from the University of Patras, Patras, Greece, in 1972, and the Ph.D. degree in applied science/electronic engineering from the University of Newcastle, Newcastle-upon-Tyne, U.K., in 1976.

He has been a Professor of electrical engineering and computer science, University of Michigan, Ann Arbor, since 1986. He was an Invited Guest of the Institute of Semiconductor Electronics, Technical University of Aachen, Aachen, Germany, in 1974.

He was a Postdoctoral Fellow with the University of Newcastle from 1976 to 1978, engaged in work on microwave semiconductor devices and circuits. In 1978, he joined the High Frequency Institute of the Technical University of Darrnstadt, Darrnstadt, Germany, as a Lecturer working on III–V devices and establishing a new semiconductor technology facility. In 1980, he worked at the Central Electronic Engineering Research Institute, Pilani, India, as UNESCO consultant. From 1980 to 1985, he was Engineer and Manager of the GaAs Monolithic Microwave Integrated Circuits (MMIC) Department, Thomson-CSF, Corbeville, France. In this capacity, he was responsible for projects on various monolithic circuits, their technology, and process evaluation. He was a Visiting Scientist of the Centre National d'Études des Télécommunications (CNET), France Telecom, Bagneux, France, from January to June 1993. Since 1986, he has been involved in research on heterostructure devices and materials at the University of Michigan. This includes the design, fabrication, and characterization of GaAs, InP-based HEMTs and HBTs, diodes for switching and mixing, GaN-based HFETs, and two-terminal devices. His research also covers microwave/millimeter-wave monolithic heterostructure integrated circuits built with such devices. His materials research covers InP and III–V Nitride-based heterostructures using metalorganic chemical vapor deposition (MOCVD) and their device applications. His work in the above areas has been reported in numerous papers and reports, and he holds six patents.

Prof. Pavlidis was awarded the European Microwave Prize for his work in InP-based monolithic integrated HEMT amplifiers in 1990. In 1991, he received the decoration of "Palme Académiques" in the order of Chevalier by the French Ministry of Education for his work in education. In 1992 and 1999, he received the Japan Society of Promotion of Science Fellowship for Senior Scientists/Professors from the Japanese Government, and in 1992, he received the Humboldt Research Award for Distinguished senior U.S. Scientists. He is the recipient of the University of Michigan 1994 Electrical Engineering and Computer Science and 1996 College of Engineering Research Excellence Awards.

Saeed Mohammadi (M'00), photograph and biography not available at the time of publication.

Jean-Luc Guyaux, photograph and biography not available at the time of publication.

Jean-Charles Garcia, photograph and biography not available at the time of publication.